

Analysis of a diffuse-photon-density wave in multiple-scattering media in the presence of a small spherical object

X. D. Zhu and Sung-po Wei

Department of Physics, University of California at Davis, Davis, California 95616-8677

Shechao Charles Feng

Department of Physics, University of California at Los Angeles, Los Angeles, California 90024-1547

Britton Chance

Department of Biochemistry and Biophysics, University of Pennsylvania, Philadelphia, Pennsylvania 19104

Received June 12, 1995; revised manuscript received August 28, 1995; accepted September 28, 1995

We present a general analysis of the sensitivity of a diffuse photon density wave in a homogeneous multiple-scattering medium to the presence of a small spherical object. From our calculations in both infinite and semi-infinite geometry we derive the charge and dipole coefficients that typify the object's most significant response. © 1996 Optical Society of America

1. INTRODUCTION

In the field of medical imaging the migration of diffuse photons in multiple-scattering media has recently received much attention.¹⁻⁴ This is due to the promising new discovery that diffuse photon flux at a tissue surface may provide sufficient information about the location and size of foreign objects and growths in otherwise normal human tissue. The idea of using diffuse photon density or flux as the basis of new noninvasive imaging tools has been proposed and studied by many groups.¹⁻⁴ Following the work of Arridge and den Outer *et al.*, Feng *et al.* reported a perturbation calculation of the change in diffuse photon density in the presence of a small spherical defect.⁵⁻⁹ They showed that the most important change, resulting from the embedment of a small spherical object in an otherwise homogeneous multiple-scattering medium, is characterized by charge and dipole terms, similar to the findings of den Outer and co-workers. These findings are most relevant to the potential application of diffuse-photon-density wave spectroscopy to, for example, early breast cancer detection.¹ In this case one is concerned mainly with tissue growths that are small compared with the overall size of a human breast and the absorption depth of the near-infrared light.¹ These authors showed that one may need only one or at most four parameters to characterize the net change of a diffuse-photon-density wave that is due to a small abnormal object in an otherwise homogeneous medium. However, in the paper by Feng *et al.*, several crucial details such as the derivation of various coefficients [Eqs. (20) and (21) of Ref. 6] and the circumstances under which they may apply were neglected. A more systematic calculation was reported recently by Boas *et al.*¹⁰ They also found numerically that as the size of an embedded object in a multiple-scattering medium decreases, the change of the

diffuse-photon-density wave (the scattered wave) becomes more isotropic, indicative of a more predominant contribution from a charge-like term. These authors stopped short of explicitly deriving the charge and dipole coefficients from their general results. In this paper we strive to fill in the gaps by making available the exact results of the scattered diffuse-photon-density wave in a single-source configuration. From the exact results we will consider a number of special situations encountered in previous studies, including the ones dealt with in Refs. 6 and 10, and we will present the appropriate charge and dipole coefficients that describe the major part of the scattered diffuse photon density wave. Our results may serve as a convenient starting point in the application of diffuse-photon-density wave spectroscopy to early tumor detection. Also significant is the fact that our results can easily be applied to cases in which more than one light source are involved.

2. DIFFUSIVE PHOTON DENSITY AND FLUX IN MULTIPLE-SCATTERING MEDIA IN THE PRESENCE OF A SMALL SPHERICAL DEFECT OBJECT: THE INFINITE GEOMETRY CASE

Consider a monochromatic point light source placed at position \mathbf{r}_0 in an infinite homogeneous multiple-scattering medium as shown in Fig. 1. It has a strength S_0 expressed in units of number of photons per second. The time-dependent diffuse-photon-number density $\Phi(\mathbf{r}, t)$ at position \mathbf{r} in the medium satisfies the diffusion equation¹¹

$$\frac{1}{c} \frac{\partial \Phi(\mathbf{r}, t)}{\partial t} - D \nabla^2 \Phi(\mathbf{r}, t) + \mu_a \Phi(\mathbf{r}, t) = S_0(t) \delta(\mathbf{r} - \mathbf{r}_0). \quad (1)$$

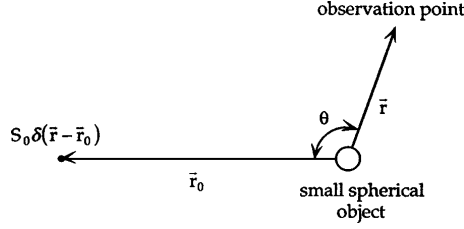


Fig. 1. Small spherical defect object with radius of curvature a embedded in an infinite multiple-scattering medium. The origin of the coordinate system overlaps the center of the object. A point light source is placed at \mathbf{r}_0 .

Here D is the diffusion constant of the medium, $D = 1/3[\mu_a + (1 - g)\mu_s]$, μ_a is the absorption coefficient (in units of inverse length), $\mu_s = 1/\ell_s$ is the scattering coefficient with ℓ_s serving as the scattering mean free path, and $g = \langle \cos \theta_{\text{scattering}} \rangle$. The quantity $\mu_{\text{tr}} \equiv (1 - g)\mu_s = 1/\ell_{\text{tr}}$ is also known as the transport scattering coefficient with ℓ_{tr} serving as the transport mean free path.¹² $c = c_0/n$ is the speed of light inside the multiple-scattering medium with a refractive index n .

We consider the general situation in which the amplitude of the point source may be modulated at a frequency Ω , i.e., $S_0 \exp(-i\Omega t)$.¹⁰ By setting Ω to zero we can reduce the result to cases in which continuous-wave sources are used. In the steady state the diffusion equation assumes the following form:

$$-\nabla^2 \Phi(\mathbf{r}, \Omega) + \left(\frac{\mu_a}{D} - \frac{i\Omega}{Dc} \right) \Phi(\mathbf{r}, \Omega) = \frac{S_0}{D} \delta(\mathbf{r} - \mathbf{r}_0). \quad (2)$$

Equation (2) is solved by the well-known function

$$\Phi_0(\mathbf{r}, \Omega) = \frac{S_0}{4\pi D} \frac{\exp(-\kappa|\mathbf{r} - \mathbf{r}_0|)}{|\mathbf{r} - \mathbf{r}_0|}, \quad (3)$$

where $\kappa^2 \equiv [(\mu_a/D) - (i\Omega/Dc)]$. The diffuse photon flux is given by

$$\mathbf{J}_0 = -D\nabla\Phi_0(\mathbf{r}, \Omega). \quad (4)$$

Now we place a small spherical object at the origin $\mathbf{r} = 0$. Its radius of curvature a is much smaller than $r_0 \equiv |\mathbf{r}_0|$. Inside the sphere the scattering parameters are denoted as D' , μ'_a , μ'_s , g' , and $\kappa' \equiv \sqrt{\mu'_a/D' - i\Omega/D'c}$.^{5,6} We are interested in the perturbation correction to $\Phi_0(\mathbf{r}, \Omega)$ at an observation point \mathbf{r} . As described in Appendix A the diffuse photon density outside the sphere takes the form

$$\Phi_{\text{out}}(\mathbf{r}, \Omega) = \Phi_0(\mathbf{r}, \Omega) + \sum_{m=0}^{\infty} B_m k_m(\kappa r) P_m(\cos \theta), \quad (5)$$

where θ is the angle between \mathbf{r}_0 and \mathbf{r} . The expansion coefficients B_m are determined from the boundary conditions that require the diffuse photon density and flux to be continuous across the surface of the sphere:

$$B_m = \frac{(-)S_0 \kappa (2m + 1) k_m(\kappa r_0)}{4\pi D} \times \left\{ \frac{\kappa D i_m(\kappa' a) [i_m(\kappa a)]^{(1)} - \kappa' D' i_m(\kappa a) [i_m(\kappa' a)]^{(1)}}{\kappa D i_m(\kappa' a) [k_m(\kappa a)]^{(1)} - \kappa' D' k_m(\kappa a) [i_m(\kappa' a)]^{(1)}} \right\}, \quad (6)$$

where $i_m(x)$ and $k_m(x)$ are the spherical modified Bessel functions and $[i_m(x)]^{(1)}$ and $[k_m(x)]^{(1)}$ are their first derivatives, respectively.¹³ It is easily verified that when the sphere is absent so that $D = D'$ and $\kappa = \kappa'$ we have $B_m = 0$ for all m . From Eq. (6) we can derive the so-called charge and dipole coefficients defined by^{5,6,8}

$$|q| = |B_0/\kappa| \quad (7)$$

$$|\mathbf{p}| = |B_1/\kappa^2|. \quad (8)$$

They correspond to the first two terms of the summation in Eq. (5) with $m = 0$ and $m = 1$, respectively. When $a \ll |\mathbf{r}_0|$ and $a \ll |\mathbf{r}|$ these two terms are the most important in Eq. (5) and in practice, as we will elaborate shortly.

The first interesting situation occurs under the following conditions: The point source is a continuous wave with $\Omega = 0$, and the multiple-scattering medium is very weakly absorbent or nonabsorbent ($|\kappa a| \ll 1$), whereas the small additional object is extremely absorbent ($|\kappa' a| \gg 1$). From Eq. (6) we find $B_0 \approx -\Phi_0(0)\kappa a$ and $B_1 \approx -|\nabla\Phi_0(0)|a^3\kappa^2$. The first two terms of the additional diffuse photon density are given by

$$\Phi_1(\mathbf{r}) \equiv \Phi_{\text{out}}(\mathbf{r}) - \Phi_0(\mathbf{r}) = \left[\frac{q_0}{r} + \frac{\mathbf{p}_0 \cdot \mathbf{r}}{r^3} (1 + \kappa r) \right] \exp(-\kappa r). \quad (9)$$

These terms correspond to a charge term and a dipole term that become exact if $|\kappa r|$ goes to zero (the non-absorbent limit). Here we omit the frequency variable (as $\Omega = 0$) to tidy up Eq. (9). The charge coefficient is given by

$$q_0 = -\Phi_0(0)a \quad (10)$$

and the dipole moment is given by

$$\mathbf{p}_0 = -\nabla\Phi_0(0)a^3, \quad (11)$$

which aims from the point source to the center of the small spherical object. This situation corresponds to that of the electrostatic response of a grounded, perfect conducting sphere in an external potential.¹⁴ A good example that illustrates the predominance of the charge and dipole terms was implicitly given by Boas and co-workers.¹⁰ As shown in Fig. 2(b) of Ref. 10, the amplitude contour of the scattered diffuse-photon-density wave from a spherical object with a radius as large as $a = 0.5$ cm is already almost isotropic at 1 to 1.5 cm from the center of the object, as expected from Eq. (9) with $\mathbf{p}_0 = 0$. The slight shift of the contour centers from the object toward the source is clearly the result of the contribution from the dipole moment \mathbf{p}_0 described by Eq. (11).

The second interesting situation occurs when both the multiple-scattering medium and the small spherical object are weakly absorbent but $|\kappa a| \ll |\kappa' a| \ll 1$. This is a relevant situation if one is interested in detecting small abnormal growths a few millimeters in diameter in the human breast or the human brain at optical wavelengths near 800 nm.¹ In this case the most important correction to the unperturbed diffusive photon density $\Phi_0(\mathbf{r})$ is again characterized by a charge term and a dipole term:

$$\Phi_1(\mathbf{r}) \approx \left[\frac{q}{r} + \frac{\mathbf{p} \cdot \mathbf{r}}{r^3} (1 + \kappa r) \right] \exp(-\kappa r). \quad (12)$$

The charge and the dipole coefficients are reduced to

$$q = -\Phi_0(0) a \left(\frac{\mu_a' a^2}{3D} \right) = q_0 \frac{\mu_a' a^2}{3D} \quad (13)$$

$$\mathbf{p} = -\nabla \Phi_0(0) a^3 \frac{D' - D}{D' + 2D} = \mathbf{p}_0 \frac{D' - D}{D' + 2D}. \quad (14)$$

This result agrees with the diagrammatic calculation by Nieuwenhuizen and van Rossum¹⁵ and originally attempted by Berkovits and Feng.¹⁶ It is noteworthy that if the small object is transparent so that $\kappa' = 0$ and $D' \rightarrow \infty$ then $q = 0$ and $\mathbf{p} = \mathbf{p}_0$. This means that there will be no charge term and that the dipole term is restored to that of a perfect absorber. This situation corresponds to that of the electrostatic response of an ungrounded, perfectly conducting sphere in an external potential.

The third interesting situation occurs when both κa and $\kappa' a$ are finite but $|(\kappa' - \kappa)a| \ll 1$ and $|(D' - D)/D| \ll 1$. The light source can be either a continuous wave or an amplitude-modulated wave. In this case we can expand the functions in Eq. (6) around κ and D and keep only the terms varying linearly with $\delta\kappa = \kappa' - \kappa$ and $\delta D = D' - D$. We find that

$$B_0 = -\Phi_0(0) \{ (\delta\kappa/\kappa) [\sinh(\kappa a) \cosh(\kappa a) - \kappa a] + (\delta D/D) [\sinh(\kappa a)/\kappa a] \times [\kappa a \cosh(\kappa a) - \sinh(\kappa a)] \} \quad (15)$$

and

$$B_1 = -\frac{3|\nabla \Phi_0(0)|}{\kappa^4 a^3} \{ (\delta\kappa/\kappa) [\kappa a \sinh(\kappa a) \cosh(\kappa a) + \kappa^2 a^2 - 2 \sinh^2(\kappa a)] \kappa^2 a^2 + (\delta D/D) [\kappa a \cosh(\kappa a) - \sinh(\kappa a)] [\kappa^2 a^2 \sinh(\kappa a) - 2\kappa a \cosh(\kappa a) + 2 \sinh(\kappa a)] \}. \quad (16)$$

The leading-order changes in the diffuse photon density are given by Eq. (12), with the charge and the dipole coefficients given by

$$q = -\frac{\Phi_0(0)}{\kappa} \{ (\delta\kappa/\kappa) [\sinh(\kappa a) \cosh(\kappa a) - \kappa a] + (\delta D/D) [\sinh(\kappa a)/\kappa a] \times [\kappa a \cosh(\kappa a) - \sinh(\kappa a)] \}, \quad (17)$$

$$\mathbf{p} = -\frac{3\nabla \Phi_0(0)}{\kappa^6 a^3} \{ (\delta\kappa/\kappa) [\kappa a \sinh(\kappa a) \cosh(\kappa a) + \kappa^2 a^2 - 2 \sinh^2(\kappa a)] \kappa^2 a^2 + (\delta D/D) [\kappa a \cosh(\kappa a) - \sinh(\kappa a)] [\kappa^2 a^2 \sinh(\kappa a) - 2\kappa a \cosh(\kappa a) + 2 \sinh(\kappa a)] \}. \quad (18)$$

We note that in the weak-absorption limit when the magnitudes of both κa and $\kappa' a$ are small compared with unity,

Eqs. (17) and (18) are simplified to

$$q = q_0 \frac{a^2(\mu_a' - \mu_a)}{3D} \quad (19)$$

$$\mathbf{p} \approx \frac{\mathbf{p}_0}{3} \left[(\delta D/D) + \frac{2}{5} (\delta\kappa/\kappa) \kappa^2 a^2 \right], \quad (20)$$

where q_0 and \mathbf{p}_0 are given by Eqs. (10) and (11). Such a perturbation limit is experimentally relevant in the case of detecting tumor growth in the human breast and the human brain in the optical wavelength range near 800 nm. Relations (19) and (20) reduce to Eqs. (13) and (14) when κa approaches zero.

For more general situations one should use both the full solution prescribed by Eq. (5), which includes multipolar terms of all orders, and the exact coefficients given by Eq. (6). Once the distribution of the diffuse photon density is determined, the photon flux can be obtained from Eq. (4).

3. DIFFUSE PHOTON DENSITY AND FLUX IN A MULTIPLE-SCATTERING MEDIUM IN THE PRESENCE OF A SMALL SPHERICAL DEFECT OBJECT: THE SEMI-INFINITE GEOMETRY CASE

It is easy to extend the results of Section 2 to situations involving semi-infinite multiple-scattering media. In particular, we consider an experimentally relevant geometry as shown in Fig. 2. The multiple-scattering region (the sample region) and the scattering-free region are separated by a flat interface located at $z = 0$. The sample region occupies the half-space with $z > 0$. We consider a light source S_0 generated by placement of a point light emitter (e.g., the tip of a light-carrying optical fiber) at $\mathbf{r}_0 = (d, 0, 0)$.¹ Aronson has shown that when the sample region and the free space are index matched, the point source is effectively located slightly inside the sample region at $\mathbf{r}_s = (d, 0, z_0)$, with $z_0 \approx 0.7\ell_{tr}$.¹⁷ We are interested in evaluating the outgoing diffuse photon flux at $\mathbf{r}_d = (0, 0, 0)$ into the scattering-free region.

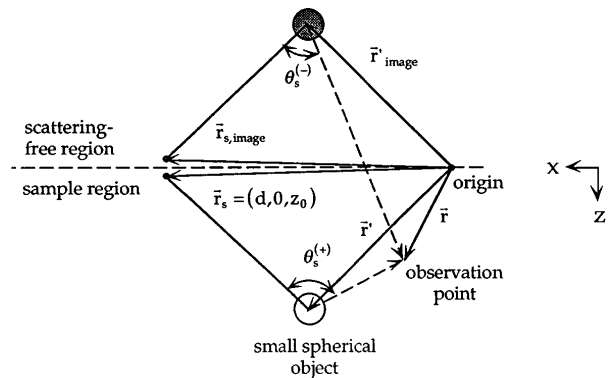


Fig. 2. Small spherical defect object with radius of curvature a embedded in a semi-infinite multiple-scattering medium (the sample region) that occupies the half-space with $z > 0$. The scattering-free region occupies the half space with $z < 0$. A point light source is placed inside the sample region at $\mathbf{r}_s = (d, 0, z_0)$. Special attention should be paid to the definitions of $\theta_s^{(+)}$ and $\theta_s^{(-)}$ that are used in Appendix B.

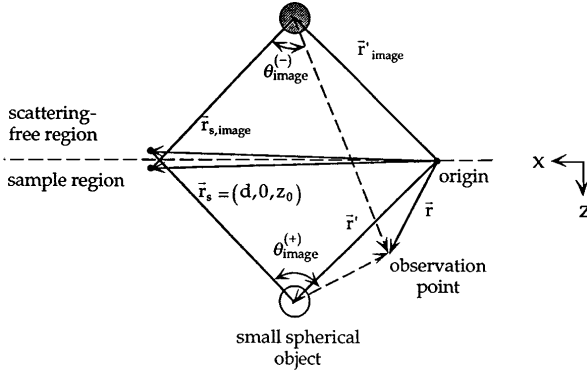


Fig. 3. Same as Fig. 2 except for the definitions of $\theta_{\text{image}}^{(+)}$ and $\theta_{\text{image}}^{(-)}$ that are used in Appendix B.

This is typically known as reflection geometry as used, for example, by Knüttel *et al.*⁹

The boundary condition at the interface can be approximated if we require that $\Phi(\mathbf{r}) = 0$ at $z = 0$ as usual. In the absence of the additional spherical object the solution to Eq. (2), $\Phi_0^{(\text{semi})}(\mathbf{r})$, is obtained simply by the method of images.¹⁴ It consists of a term $\Phi_{0,\text{orig}}(\mathbf{r})$ induced by the original source at $\mathbf{r}_s = (d, 0, z_0)$ and a term $\Phi_{0,\text{image}}(\mathbf{r})$ induced by the image of the original source at $\mathbf{r}_{s,\text{image}} = (d, 0, -z_0)$:

$$\begin{aligned} \Phi_0^{(\text{semi})}(\mathbf{r}) &= \Phi_{0,\text{orig}}(\mathbf{r}) + \Phi_{0,\text{image}}(\mathbf{r}) \\ &= \frac{S_0}{4\pi D} \frac{\exp(-\kappa|\mathbf{r} - d\hat{x} - z_0\hat{z}|)}{|\mathbf{r} - d\hat{x} - z_0\hat{z}|} \\ &\quad + \frac{(-)S_0}{4\pi D} \frac{\exp(-\kappa|\mathbf{r} - d\hat{x} + z_0\hat{z}|)}{|\mathbf{r} - d\hat{x} + z_0\hat{z}|} \\ &\approx \frac{2zz_0S_0(1 + \kappa|\mathbf{r} - d\hat{x}|)\exp(-\kappa|\mathbf{r} - d\hat{x}|)}{4\pi D|\mathbf{r} - d\hat{x}|^3}. \end{aligned} \quad (21)$$

When a small spherical object is added at $\mathbf{r}' = (x', y', z')$ in the sample region, as shown in Fig. 2, the leading-order change in the diffuse photon density is described by the charge and dipole responses of the object at $\mathbf{r}' = (x', y', z')$ and the responses of the images of these charge and dipole responses at $\mathbf{r}'_{\text{image}} = (x', y', -z')$:

$$\begin{aligned} \Phi_1^{(\text{semi})}(\mathbf{r}) &\approx q^{(\text{semi})} \left[\frac{\exp(-\kappa|\mathbf{r} - \mathbf{r}'|)}{|\mathbf{r} - \mathbf{r}'|} - \frac{\exp(-\kappa|\mathbf{r} - \mathbf{r}'_{\text{image}}|)}{|\mathbf{r} - \mathbf{r}'_{\text{image}}|} \right] \\ &\quad + p_x^{(\text{semi})}(x - x') \left[\frac{(1 + \kappa|\mathbf{r} - \mathbf{r}'|)\exp(-\kappa|\mathbf{r} - \mathbf{r}'|)}{|\mathbf{r} - \mathbf{r}'|^3} \right. \\ &\quad \left. - \frac{(1 + \kappa|\mathbf{r} - \mathbf{r}'_{\text{image}}|)\exp(-\kappa|\mathbf{r} - \mathbf{r}'_{\text{image}}|)}{|\mathbf{r} - \mathbf{r}'_{\text{image}}|^3} \right] \\ &\quad + p_z^{(\text{semi})} \left[\frac{(z - z')(1 + \kappa|\mathbf{r} - \mathbf{r}'|)\exp(-\kappa|\mathbf{r} - \mathbf{r}'|)}{|\mathbf{r} - \mathbf{r}'|^3} \right. \\ &\quad \left. + \frac{(z + z')(1 + \kappa|\mathbf{r} - \mathbf{r}'_{\text{image}}|)\exp(-\kappa|\mathbf{r} - \mathbf{r}'_{\text{image}}|)}{|\mathbf{r} - \mathbf{r}'_{\text{image}}|^3} \right]. \end{aligned} \quad (22)$$

The contributions from the higher-order multipole moments can be similarly derived, as shown in Appendix B. They are negligible in the present case when $a \ll |\mathbf{r}_0|$ and

$a \ll |\mathbf{r}|$. The numerical results of Boas and co-workers demonstrated that the contributions may be negligible even when $a \leq (1/2 \sim 1/3)|\mathbf{r}|$ and $a \leq (1/2 \sim 1/3)|\mathbf{r}_0|$.¹⁰ The charge and the dipole moments for the semi-infinite geometry are the respective sums of the charge and the dipole moments induced by the original point source at $\mathbf{r}_s = (d, 0, z_0)$ and its image at $\mathbf{r}_{s,\text{image}} = (d, 0, -z_0)$. For example, if the small spherical defect object is extremely absorbent while the multiple-scattering medium is very weakly absorbent we have the familiar result

$$q_0^{(\text{semi})} = -\Phi_0^{(\text{semi})}(\mathbf{r}')a \quad (23)$$

$$\mathbf{p}_0^{(\text{semi})} = -\nabla\Phi_0^{(\text{semi})}(\mathbf{r}')a^3, \quad (24)$$

where $\Phi_0^{(\text{semi})}(\mathbf{r})$ is given by Eq. (21).

If both the spherical object and the multiple-scattering medium are weakly absorbent, the charge coefficient is reduced to

$$q^{(\text{semi})} \approx -\frac{\Phi_0^{(\text{semi})}(\mathbf{r}')a^3(\mu_a' - \mu_a)}{3D} \quad (25)$$

and the dipole coefficient to

$$\mathbf{p}^{(\text{semi})} \approx -\frac{\nabla\Phi_0^{(\text{semi})}(\mathbf{r}')a^3}{3} \left[\left(\frac{D' - D}{D} \right) + \frac{2}{5} \left(\frac{\kappa' - \kappa}{\kappa} \right) \kappa^2 a^2 \right]. \quad (26)$$

The photon flux at the observation point $\mathbf{r}_d = (0, 0, 0)$ is obtained from Eq. (4). It is simply the near-field intensity of the output light, which can be measured either directly with close-contact fiber optics or indirectly with conventional imaging optics. In the absence of the small spherical object we have

$$\mathbf{J}_0 = -D\nabla\Phi_0^{(\text{semi})}(\mathbf{r})|_{\mathbf{r}=0} \approx -\frac{S_0z_0(1 + \kappa d)\exp(-\kappa d)}{2\pi d^3} \hat{z}, \quad (27)$$

and the flux flows from the sample region to the scattering-free region along $-\hat{z}$. Since the diffuse photon density vanishes at the interface the diffuse photon flux should have only a z component. In the presence of the small spherical object an additional diffuse photon flux arises from $\Phi_1^{(\text{semi})}(\mathbf{r})$. It has a component from the charge term,

$$\mathbf{J}_q = -\frac{2Dq^{(\text{semi})}z'(1 + \kappa r')\exp(-\kappa r')}{r'^3} \hat{z}, \quad (28)$$

and a component from the dipole term,

$$\begin{aligned} \mathbf{J}_p &= \frac{2Dz'(\mathbf{p}^{(\text{semi})} \cdot \mathbf{r}')}{r'^5} (3 + 3\kappa r' + \kappa^2 r'^2)\exp(-\kappa r') \hat{z} \\ &\quad - \frac{2Dp_z^{(\text{semi})}(1 + \kappa r')\exp(-\kappa r')}{r'^3} \hat{z}. \end{aligned} \quad (29)$$

The ratio of the magnitudes of these two components is given roughly by $J_q/J_p \approx q^{(\text{semi})}r'/p^{(\text{semi})}$. In the limit when the small object is strongly absorbent we have

$$\frac{J_q}{J_p} \approx \frac{r'^2}{a^2} \gg 1, \quad (30)$$

and therefore one has to be concerned only with \mathbf{J}_q . If the small object is not strongly absorbent, the appropriate expression for \mathbf{J}_q should be

$$\mathbf{J}_q \approx \frac{2\Phi_0^{(\text{semi})}(\mathbf{r}')a^3(\mu_{a'} - \mu_a)z'(1 + \kappa r')\exp(-\kappa r')}{3r'^3} \hat{z}. \quad (31)$$

It is linearly dependent on the absorption coefficient of the small object.

4. CONCLUSION

We have calculated analytically the changes in diffuse photon density and flux that are due to the inclusion of a small spherical defect object in an otherwise homogeneous multiple-scattering medium. We reiterate that the most important contribution to the scattered diffuse-photon-density wave is from a charge term and a dipole term. The exact calculations and the charge and dipole coefficients are provided for the single pointlike source configuration in both infinite and semi-infinite geometry. The results can be applied easily to cases in which multiple point sources or extended sources are used. In fact, as has been suggested by Schmitt, Knüttel, Knutson, Chance and others,⁹ by using two pointlike, amplitude-modulated sources with opposite phases it is possible to cancel the large contribution from $\mathbf{J}_0 = -D\nabla\Phi_0^{(\text{semi})}$ while maintaining the essential contribution from \mathbf{J}_q .^{5,9} This significantly enhances the sensitivity and the spatial resolution of diffuse photon flux as a probe to small objects in multiple-scattering media. Our results should be useful to many of the ongoing efforts toward the use of diffuse photon densities to obtain image information about objects embedded in human tissues or other realistic multiple-scattering systems.

APPENDIX A: DERIVATION OF THE EXPANSION COEFFICIENTS B_m IN EQ. (5) FOR INFINITE GEOMETRY

We select the origin to be at the center of the small spherical object. Inside the sphere we express the solution to Eq. (2) as an infinite series,

$$\Phi_{\text{in}}(\mathbf{r}) = \sum_{m=0}^{\infty} A_m i_m(\kappa r) P_m(\cos \theta). \quad (A1)$$

Outside the sphere

$$\Phi_{\text{out}}(\mathbf{r}) = \Phi_0(\mathbf{r}) + \sum_{m=0}^{\infty} B_m k_m(\kappa r) P_m(\cos \theta). \quad (A2)$$

We now expand $\Phi_0(\mathbf{r})$ in Eq. (3) by using the well-known identity¹⁸

$$\Phi_0(\mathbf{r}) = \frac{S_0 \kappa}{4\pi D} \sum_{m=0}^{\infty} (2m+1) i_m(\kappa r) k_m(\kappa r_0) P_m(\cos \theta) \quad (A3)$$

and rewrite the solution outside the sphere as

$$\Phi_{\text{out}}(\mathbf{r}) = \sum_{m=0}^{\infty} \left[B_m k_m(\kappa r) + \frac{(2m+1)\kappa S_0 k_m(\kappa r_0)}{4\pi D} i_m(\kappa r) \right] \times P_m(\cos \theta). \quad (A4)$$

We now require that the total diffusive photon density and the normal component of the photon flux be continuous across the surface of the sphere (the boundary conditions):

$$\Phi_{\text{in}}(\mathbf{r})|_{r=a} = \Phi_{\text{out}}(\mathbf{r})|_{r=a}, \quad (A5)$$

$$D' \frac{\partial \Phi_{\text{in}}(\mathbf{r})}{\partial r} \Big|_{r=a} = D \frac{\partial \Phi_{\text{out}}(\mathbf{r})}{\partial r} \Big|_{r=a}. \quad (A6)$$

Inserting Eqs. (A1) and (A4) into Eqs. (A5) and (A6), respectively, we obtain

$$A_m = \frac{(-)S_0 \kappa (2m+1) k_m(\kappa r_0)}{4\pi D} \times \left\{ \frac{\kappa D k_m(\kappa a) [i_m(\kappa a)]^{(1)} - \kappa D i_m(\kappa a) [k_m(\kappa a)]^{(1)}}{\kappa D i_m(\kappa' a) [k_m(\kappa a)]^{(1)} - \kappa' D' k_m(\kappa a) [i_m(\kappa' a)]^{(1)}} \right\}, \quad (A7)$$

$$B_m = \frac{(-)S_0 \kappa (2m+1) k_m(\kappa r_0)}{4\pi D} \times \left\{ \frac{\kappa D i_m(\kappa' a) [i_m(\kappa a)]^{(1)} - \kappa' D' i_m(\kappa a) [i_m(\kappa' a)]^{(1)}}{\kappa D i_m(\kappa' a) [k_m(\kappa a)]^{(1)} - \kappa' D' k_m(\kappa a) [i_m(\kappa' a)]^{(1)}} \right\}. \quad (A8)$$

APPENDIX B: DERIVATION OF THE EXPANSION COEFFICIENTS OF $\Phi_1^{(\text{semi})}(\mathbf{r})$ IN EQ. (22) TO ALL ORDERS IN SEMI-INFINITE GEOMETRY

In semi-infinite geometry, as shown in Figs. 2 and 3, a boundary condition exists in which the total diffuse photon density vanishes at the interface $z = 0$. Thus the change in the diffuse photon density can be obtained by the method of images. It is convenient to consider separately the effects of the original source at $\mathbf{r}_s = (d, 0, z_0)$ and its image at $\mathbf{r}_{s,\text{image}} = (d, 0, -z_0)$. $\Phi_1^{(\text{semi})}(\mathbf{r})$ is then partitioned into a term $\Phi_{1,s}^{(\text{semi})}(\mathbf{r})$ corresponding to the original source and a term $\Phi_{1,\text{image}}^{(\text{semi})}(\mathbf{r})$ corresponding to the image of the original source.

We first examine $\Phi_{1,s}^{(\text{semi})}(\mathbf{r})$. Without the interface $\Phi_{1,s}^{(\text{semi})}(\mathbf{r})$ is simply given by the expression similar to Eq. (5):

$$\Phi_1^{(\text{infinite})}(\mathbf{r}) = \sum_{m=0}^{\infty} B_m^{(s)} k_m(\kappa |\mathbf{r} - \mathbf{r}'|) P_m[\cos \theta_s^{(+)}] \quad (B1)$$

and the expansion coefficients

$$B_m^{(s)} = \frac{(-)S_0 \kappa (2m+1) k_m(\kappa |\mathbf{r}_s - \mathbf{r}'|)}{4\pi D} \times \left\{ \frac{\kappa D i_m(\kappa' a) [i_m(\kappa a)]^{(1)} - \kappa' D' i_m(\kappa a) [i_m(\kappa' a)]^{(1)}}{\kappa D i_m(\kappa' a) [k_m(\kappa a)]^{(1)} - \kappa' D' k_m(\kappa a) [i_m(\kappa' a)]^{(1)}} \right\}. \quad (B2)$$

With the interface an additional term arises that must satisfy the homogeneous diffusion equation in the sample region. Following the principle of the image method, the additional term in effect originates from the image of the small spherical object with the interface as the mirror plane. As a result it is easily verified that

$$\Phi_{1,s}^{(\text{semi})}(\mathbf{r}) = \sum_{m=0}^{\infty} B_m^{(s)} \{ k_m(\kappa |\mathbf{r} - \mathbf{r}'|) P_m[\cos \theta_s^{(+)}] - k_m(\kappa |\mathbf{r} - \mathbf{r}'_{\text{image}}|) P_m[\cos \theta_s^{(-)}] \}. \quad (B3)$$

The definition of the angles as shown in Fig. 2, and $B_m^{(s)}$ is given by Eq. (B2). The response of the small spherical

object to the image of the original source $\Phi_{1,\text{image}}^{(\text{semi})}(\mathbf{r})$ can now easily be recorded with the relevant angles defined in Fig. 3:

$$\Phi_{1,\text{image}}^{(\text{semi})}(\mathbf{r}) = \sum_{m=0}^{\infty} B_m^{(\text{image})} \{ k_m(\kappa|\mathbf{r} - \mathbf{r}'|) P_m[\cos \theta_{\text{image}}^{(+)}] - k_m(\kappa|\mathbf{r} - \mathbf{r}'_{\text{image}}|) P_m[\cos \theta_{\text{image}}^{(-)}] \}. \quad (\text{B4})$$

Here

$$B_m^{(\text{image})} = \frac{(+)\mathcal{S}_0 \kappa (2m+1) k_m(\kappa|\mathbf{r}_{s,\text{image}} - \mathbf{r}'|)}{4\pi D} \times \left\{ \frac{\kappa D i_m(\kappa'a) [i_m(\kappa a)]^{(1)} - \kappa' D' i_m(\kappa a) [i_m(\kappa'a)]^{(1)}}{\kappa D i_m(\kappa'a) [k_m(\kappa a)]^{(1)} - \kappa' D' k_m(\kappa a) [i_m(\kappa'a)]^{(1)}} \right\}. \quad (\text{B5})$$

Finally, the total change in diffuse photon density in semi-infinite geometry is expressed as

$$\begin{aligned} \Phi_1^{(\text{semi})}(\mathbf{r}) &= \Phi_{1,s}^{(\text{semi})}(\mathbf{r}) + \Phi_{1,\text{image}}^{(\text{semi})}(\mathbf{r}) \\ &= \sum_{m=0}^{\infty} B_m^{(s)} \{ k_m(\kappa|\mathbf{r} - \mathbf{r}'|) P_m[\cos \theta_s^{(+)}] - k_m(\kappa|\mathbf{r} - \mathbf{r}'_{\text{image}}|) P_m[\cos \theta_s^{(-)}] \} \\ &\quad + \sum_{m=0}^{\infty} B_m^{(\text{image})} \{ k_m(\kappa|\mathbf{r} - \mathbf{r}'|) P_m[\cos \theta_{\text{image}}^{(+)}] - k_m(\kappa|\mathbf{r} - \mathbf{r}'_{\text{image}}|) P_m[\cos \theta_{\text{image}}^{(-)}] \}. \quad (\text{B6}) \end{aligned}$$

The first two terms from the two preceding summations are the most important in the limit that $a \ll |\mathbf{r}_0|$ and $a \ll |\mathbf{r}|$. They can be rewritten in terms of charge and dipole responses as described in Eq. (22).

ACKNOWLEDGMENTS

This work was supported in part by the U.S. Office of Naval Research under grant N00014-92-J-4004, by the U.S. Department of Energy under grant DE-FG03-88ER45, and by the U.S. Army Research Office under grant DAAH04-94-G-035.

Correspondence should be conducted with X. D. Zhu at the address on the title page; telephone 916-752-4689.

REFERENCES

1. A. Yodh and B. Chance, "Spectroscopy and imaging with diffusing light," *Physics Today* **48**, 34–40 (1995).
2. B. Chance and R. R. Alfano, eds., *Photon Migration and Imaging in Random Media and Tissues*, Proc. SPIE **1888** (1993).
3. R. R. Alfano, ed., *Advances in Optical Imaging and Photon Migration*, Vol. 21 of 1994 OSA Technical Digest Series (Opt. Soc. of Am., Washington, D.C., 1994).
4. B. Chance and R. R. Alfano, eds., *Optical Tomography, Photon Migration, and Spectroscopy of Tissue and Model Media: Theory, Human Studies, and Instrumentation*, Proc. SPIE **2389** (1995).
5. S. Feng, F. Zeng, and B. Chance, "Monte Carlo simulations of photon migration path distribution in multiple scattering media," in *Photon Migration and Imaging in Random Media and Tissues*, B. Chance and R. R. Alfano, eds., Proc. SPIE **1888**, 78–89 (1993).
6. Shechao Feng, Fan-An Zeng, and B. Chance, "Photon migration in the presence of a single defect—a perturbation analysis," *Appl. Opt.* **34**, 3826–3837 (1995).
7. S. R. Arridge, M. Schweiger, and D. T. Delpy, "Iterative reconstruction of new infra-red absorption images," in *Inverse Problems in Scattering and Imaging*, M. A. Fiddy, ed., Proc. SPIE **1767**, 372–383 (1992).
8. P. N. den Outer, Th. M. Nieuwenhuizen, and A. Lagendijk, "Location of objects in multiple-scattering media," *J. Opt. Soc. Am. A* **10**, 1209–1218 (1993).
9. J. M. Schmitt, A. Knüttel, and J. R. Knutson, "Interference of diffusive light waves," *J. Opt. Soc. Am. A* **9**, 1832–1843 (1992); A. Knüttel, J. M. Schmitt, and J. R. Knutson, "Spatial localization of absorbing bodies by interfering diffusive photon-density waves," *Appl. Opt.* **32**, 381–389 (1993); A. Knüttel, J. M. Schmitt, R. Barnes, and J. R. Knutson, "Acoustic-optic scanning and interfering photon density waves for precise localization of an absorbing (or fluorescent) body in a turbid medium," *Rev. Sci. Instrum.* **64**, 638–644 (1993); B. Chance, K. Kang, L. He, J. Weng, and E. Sevick, "Highly sensitive object location in tissue models with linear in-phase and anti-phase multi-element optical arrays in one and two dimensions," *Proc. Natl. Acad. Sci. USA (Medical Sciences)* **90**, 3423–3427 (1993).
10. D. A. Boas, M. A. O'Leary, B. Chance, and A. G. Yodh, "Scattering of diffuse photon density waves by spherical inhomogeneities within turbid media: analytic solution and applications," *Proc. Natl. Acad. Sci. USA* **91**, 4887–4891 (1994).
11. A. Ishimaru, *Wave Propagation and Scattering in Random Media* (Academic, New York, 1978).
12. H. C. van de Hulst, *Multiple Light Scattering* (Academic, New York, 1980), Vols. I and II; M. B. van der Mark, M. P. van Albada, and A. Lagendijk, "Light scattering in strongly scattering media; Multiple scattering and weak localization," *Phys. Rev. B* **37**, 3575–3592 (1988).
13. G. Arfken, *Mathematical Methods for Physicists*, 2nd ed. (Academic, New York, 1970), pp. 531–532.
14. J. D. Jackson, *Classical Electrodynamics* (Wiley, New York, 1975).
15. Th. M. Nieuwenhuizen and M. C. W. van Rossum, "Role of a single scatterer in a multiple scattering medium," *Phys. Lett. A* **177**, 102–106 (1993).
16. R. Berkovits and Shechao Feng, "Theory of speckle-pattern tomography in multiple-scattering media," *Phys. Rev. Lett.* **65**, 3120–3123 (1990).
17. R. Aronson, "Extrapolation distance for diffusion of light," in *Photon Migration and Imaging in Random Media and Tissues*, B. Chance and R. R. Alfano, eds., Proc. SPIE **1888**, 297–305 (1993).
18. I. S. Grashsteyn and I. M. Ryzhik, *Table of Integrals, Series, and Products*, 5th ed., A. Jeffrey, ed. (Academic, New York, 1994).